First results on the behaviour of solar wind protons and alphas in the Stream Interaction Region in solar cycle 23 and 24

Yogesh,[1,2]★ D. Chakrabarty[1], and Nandita Srivastava[3]
[1]Physical Research Laboratory, Navrangpura, Ahmedabad 380009, India
[2]Indian Institute of Technology-Gandhinagar, Gandhinagar 382055, India
[3]Udaipur Solar Observatory, Physical Research Laboratory, Udaipur -313001, India

Accepted XXX. Received YYY; in original form ZZZ

ABSTRACT

Although the enhancements in the alpha-proton ratio in the solar wind (expressed as $A_{He} = N_a/N_p * 100$) in the Interplanetary Coronal Mass Ejections (ICMEs) have been studied in the past, A_{He} enhancements at the stream interface region received very little attention so far. In this letter, by extensively analyzing the stream interaction region (SIR) events observed in solar cycle 23 and 24, we show that the stream interface of alphas starts separating out from that of protons from the minimum of solar cycle 23. We show that more alpha particles are distributed towards higher pitch angles as compared to protons in the fast wind region compared to background solar wind. By analysing the differential velocities of alphas and protons, we also show that the faster alpha particles accumulate near the fast wind side of the stream interface region leading to enhancement of A_{He}. The investigation brings out, for the first time, the salient changes in A_{He} in SIRs for the two solar cycles and highlight the important roles of pitch angle and differential velocities of alpha and protons in the fast wind region for the changes in A_{He} in SIRs.

Key words: Solar wind – Sun: abundances – Sun: magnetic fields – Sun: activity

1 INTRODUCTION

The stream interaction regions (SIRs) are large-scale and long lasting structures in the Interplanetary (IP) medium. SIRs influence the dynamics of near-earth solar wind properties and hence, associated space weather impact. The SIRs are formed by the interaction of high-speed solar wind stream with the preceding slow solar wind. The increase in plasma density, magnetic field strength, and plasma pressure indicate compressed plasma in the stream interaction region. SIRs have three parts - slow wind region, stream interface region, and fast wind region. The stream interface (SI) is usually characterized by an abrupt drop in density, an increase in the temperature/pressure, and a change in velocity with a large gradient at 1 au (Burlaga 1974; Belcher & Davis 1971). Earlier researchers have studied the changes in solar wind plasma parameters, i.e., density, magnetic field, dynamic pressure, etc. (Richardson 2018, and references therein) associated with SIR. However, there are very few studies (e.g. Gosling et al. 1978; Ďurovcová et al. 2019) on how stream interaction regions would alter the solar wind plasma composition in general and alpha-proton ratio (expressed as $A_{He} = N_a/N_p * 100$) in particular. This is probably because large enhancement in A_{He} in SIRs is rare unlike interplanetary Coronal Mass Ejections (ICMEs) wherein significant enhancements in A_{He} are observed quite frequently (Richardson & Cane 2010; Fu et al. 2020; Yogesh et al. 2022, etc.). Nevertheless, how A_{He} varies across the stream interface can be very useful in characterising SIR structures and to evaluate the space weather impact.

It is also worthwhile to mention here that A_{He} can provide indication about the source region of the solar wind (e.g., Borrini et al. 1982; Kasper et al. 2007). It is also known that the although A_{He} is 8% in the photosphere, it gets depleted in corona and solar wind and gets fixed at a 4-5% level (Laming 2004). Yogesh et al. (2021) showed that this scenario got changed in solar cycle 24 when A_{He} shifted towards lower values (2-3%) indicating changes in the helium processing in the corona in the last cycle. Further, A_{He} varies in solar wind according to solar wind speed and the solar activity level (Kasper et al. 2007; Alterman & Kasper 2019; Yogesh et al. 2021). Usually, the fast wind shows higher A_{He} as compared to the slow wind. A_{He} values are more variable in slow solar wind, whereas it does not vary significantly in the case of fast wind. Yogesh et al. (2022) also showed that the possible interplay of chromospheric evaporation and gravitational settling determines the enhanced A_{He} level in ICMEs reported earlier (e.g. Borrini et al. 1982; Fu et al. 2020, etc.). However, very little has been reported for the A_{He} variations in SIR. It was thought earlier that changes (generally increase) in helium abundance in SIR structures are only because of the transition in the type of solar wind (Gosling et al. 1978; Wimmer-Schweingruber et al. 1997). Gosling et al. (1978) also showed that alpha flow speeds relative to protons change abruptly at the interface. Recently, Ďurovcová et al. (2019) suggested that the pitch angle and velocity of alphas in the proton frame are important factors to be accounted to explain the enhancement in A_{He} in SIRs.

In this letter, we explore how the above suggestions play out for a large number of SIR events spanning over solar cycle 23 and 24 (henceforth, SC23 and SC24) in the context of slow/fast wind and solar maxima/minima. This has not been attempted so far.

★ E-mail: yphy22@gmail.com

2 DATA AND SELECTION OF SIR EVENTS

For the present investigation, we have used the Solar Wind Experiment (SWE) data on-board the WIND spacecraft (Ogilvie et al. 1995). The dataset has a resolution of approximately 92s. The magnetic field measurements are taken from the Magnetic Field Investigation experiment (Lepping et al. 1995).

The SIR events are taken from the catalogue compiled in Chi et al. (2018). The details regarding the selection of events and the start and end times of the events at the satellite location can be found in Chi et al. (2018) and references therein. This catalogue contains 866 SIR events observed during 1995 to 2016. We have removed the events which do not have continuous coverage of data. The SIR events, having possible mix-up with ICMEs within one day before the start time and one day after the end time, are also removed to make sure that only pure SIR events are considered. The ICME events are taken from the Richardson & Cane catalogue (Richardson & Cane 2010). The above criteria lead to 436 events that are used eventually for the present investigation.

We have divided the SIR events into four categories, i.e., SC23 minima (1996-1998, 2006-2009), SC23 maxima (1999-2005), SC24 minima (2010-2011, 2016), and SC24 maxima (2012-2015). Note, SIR events beyond 2016 are not available in this catalogue making the number of SIR events considered in SC24 much less compared to SC23. Nevertheless, by considering identical number of SIR events, we have verified (see supplementary figure S1 and compare with figure 4) that the scientific inferences reported in this work remain invariant. Therefore, in this work, we exploit the full available database.

3 RESULTS AND DISCUSSIONS

3.1 Superposed Epoch Analysis (SPA) of the total events during solar maxima and minima

Figure 1 shows the superposed epoch analysis (SPA) of the SIR events used in this work. The cadence of data is changed from the 92s to 2 minutes to generate the SPA. The stream interface (SI) is the boundary between the slow and fast wind. Henceforth, the slow wind side of SI will be referred to as the Slow Wind Region (SWR), and the fast wind side will be described as the Fast Wind Region (FWR).

The change in the magnetic field, number density, and velocity can be observed in the SPA (Figure 1). The change in East-West flow angle (ϕ) is a good indicator for SI identification (Mayank et al. 2022; Rout et al. 2017). An important point that emerges from this figure is that the difference between the scaled proton number density (Scaled density = <N> =(n - nmin)/(nmax - nmin)) and scaled alpha density show very high correlation (See figure 1) with the East-West flow angle (ϕ). This differential scaled density also suggests that the pile-up of protons is dominant over alpha in SWR, whereas the alphas pile-up dominates towards FWR. Therefore, it becomes apparent from the SPA that this differential pile-up is the primary cause of relative enhancement of A_{He} in the FWR of SIRs. The possible reasons for this differential pile-up and the variations in A_{He} in minima and maxima of SC23 and SC24 are taken up in the ensuing sections.

3.2 Superposed Epoch Analysis (SPA) of number densities of alphas and protons in SC23 and SC24

In this section, we show the SPA of the number density of alpha and proton (N_a and N_p) corresponding to maxima and minima of SC23 and SC24 (Figure 2). The stream interface (dashed black line) is used as the zero-epoch time. The duration of 20 hours before and 20 hours after the zero-epoch time is shown. The variations in protons and alphas are shown in red and blue color respectively, with one sigma error bar. The red and blue dashed vertical lines represent the peak value of proton number density towards SWR and the peak alpha number density towards FWR.

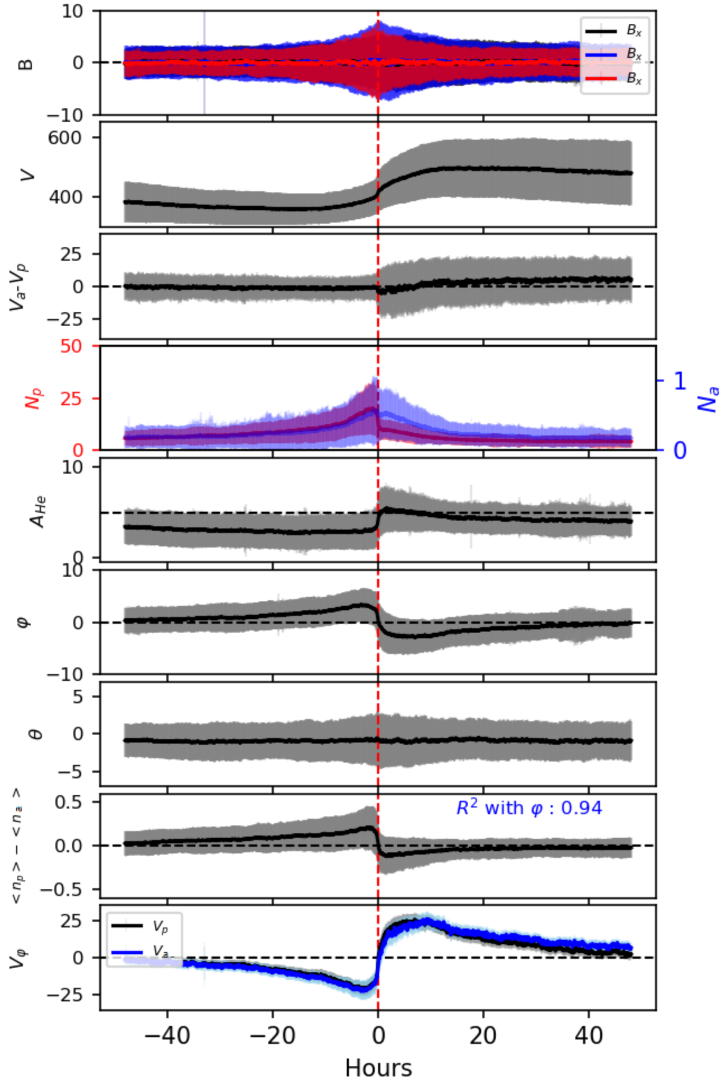

Figure 1. Superposed epoch analysis (SPA) of the 436 SIR events. The red dashed line in both panels is the epoch time. The stream interface is chosen as the epoch time. The upper seven rows of each panel show the magnetic field components (B_x, B_y, B_z), velocity (V), the difference between the alpha and proton velocities (V_a - V_p), number density of alpha and proton (N_a, N_p), Helium abundance (A_{He}), East-West GSE bulk Flow Angle (ϕ) and North-South flow angle (θ). The seventh row shows the difference between scaled proton number density (Scaled density = <N> =(n-n_{min})/(n_{max}-n_{min})) and scaled alpha number density (<N_p> - <N_a>). The eighth row shows the East-West velocity of alphas and protons ($V_\phi(a)$, $V_\phi(p)$). The ϕ and V_ϕ are good indicators for the change in the solar wind type, i.e., from slow to the fast wind. Note, R^2 (coefficient of determination) between <N_p> - <N_a> and ϕ is very high (more than 90%). This suggests that the proton pile-up dominates slow wind, whereas the alpha pile-up dominates fast wind.

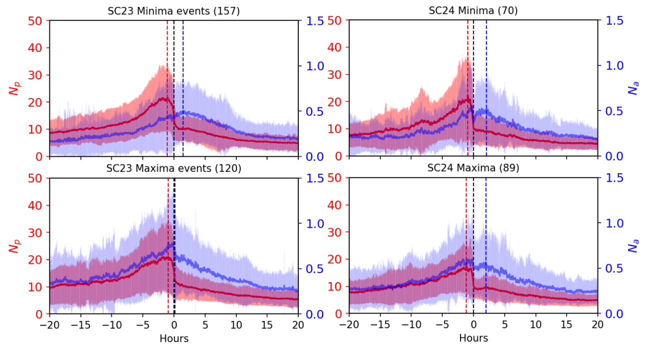

Figure 2. SPA of number densities of alphas (blue) and protons (red) in SC23 and SC24 are shown with one sigma error bar for SC23 minima, SC24 maxima, SC24 minima, and SC24 maxima. The number of events considered are also mentioned at the top of each panel. The dashed black, red, and blue vertical lines represent the stream interface (SI), the peak value of proton density towards the SWR, and the peak value of alpha density towards the FWR, respectively. The additional peaks of alpha particles towards fast wind (in SC23 minimum and SC24) suggest the differential behavior between the alphas and protons across SI.

It can be observed from Figure 2 that alphas have distinct additional SIs during SC23 minima and in SC24 (minima and maxima)and this feature seems to be absent in SC23 maxima. In addition, there is no abrupt decline in the alpha number density similar to proton density across the SI. This suggests that an enhanced helium abundance can be expected in the FWR of SIRs. It is now known that SC24 is a weaker cycle and the declining solar activity could be observed from the SC23 minima (deep minimum) itself while the maximum of SC23 was relatively stronger (Hathaway 2015). Therefore, it appears that the enhanced helium abundance at the SWR of SC23 maxima is associated with the SC23 solar activity.

Ďurovcová et al. (2019) considered the SIRs as analogous to a magnetic mirror assembly. The important parameters which control the motion of charged particles in curved magnetic fields are the pitch angle and the velocity of ions. We have evaluated how these important parameters, i.e., pitch angle and velocity difference, affect the alpha and proton number density for different phases of SC23 and SC24. It can be noted from Figure 2 that the behavior of alphas and protons are different in the SWR and FWR of SIR. Therefore, these regions are investigated individually in the upcoming subsections.

3.3 Pitch angle distribution

The pitch angle is calculated for protons and alphas as follows:

$$Pitch\ Angle\ (PA) = cos^{-1}\left(\frac{\vec{B}.\vec{V}}{|\hat{B}||\hat{V}|}\right) \quad (1)$$

Here B is the magnetic field strength and V is the velocity. The pitch angle distribution from 0^o to 90^o is only considered here and this ensured by taking modulus in the denominator. This is done as the pitch angle distribution between 90^o to 180^o is expected to be the mirror image of the pitch angle distribution between 0^o to 90^o. Figure 3 shows the pitch angle distribution in minima and maxima of SC23 and SC24 in SWR. To understand the effect of the stream interaction, the pitch angle distribution of SIRs is compared with the pitch angle distribution of the background slow and fast winds in absence of SIR. Solar wind velocities less than 400 km/s and higher than 500 km/s are used to construct the references for the slow and fast background wind respectively. The solar wind having velocities between 400-500 km/s is not considered to maintain the sanctity of the references. In addition, the ICME events are also removed from the data to estimate the background references. Note the references are constructed based on data during 1996-2016 to make it consistent with the SIR catalog. The red and blue colors are for protons and alphas respectively.

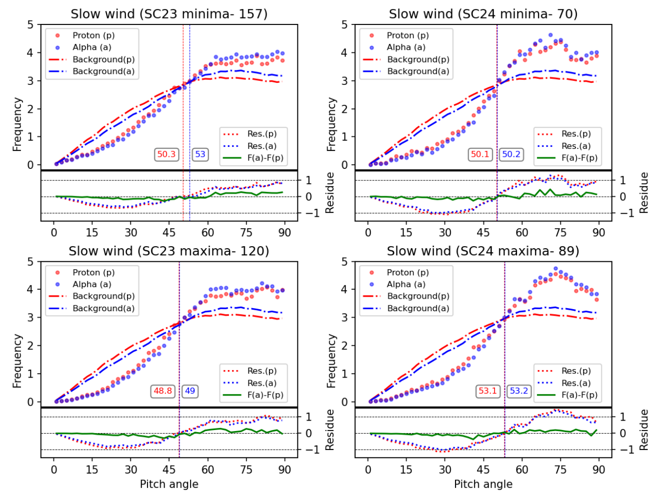

Figure 3. The pitch angle distributions for minima and maxima for SC23 and 24 are shown only for the slow wind region (SWR). The red and blue colors are used for protons and alphas, respectively. The upper part of each panel shows the pitch angle distribution for SWR of SIR and slow background wind. The lower part of each panel shows the difference between SIR pitch angle distribution and the background slow wind. The green color indicates the difference between alpha and proton pitch angle distribution for SWR.

3.3.1 Slow Wind Region (SWR)

In each panel of figure 3, the upper part shows the pitch angle distribution (of protons and alphas) in SWR of SIR in dotted lines whereas the dotted dashed lines capture the pitch angle distributions for the background wind. The dashed vertical lines show the cross-over of the SWR of SIR and the background pitch angle distributions. The lower part of each panel shows the difference between the pitch angle distributions in SWR of SIR and background slow solar wind. The green line shows the difference or residual between the pitch angle distributions of alphas and protons in the SWR of SIR.

A few important points can be noted from Figure 3. A part of the lower pitch angle (before the crossover) distribution seems to have shifted towards the higher values (after the crossover). This shift seems to maximize in the maxima of the SC24. The crossover point is nearly at 50^o in SC23 and SC24. The alphas and protons have similar crossover points except for SC23 minima wherein a difference of 2.7^o is noticed. The SC24 maxima shows the highest shift of particles from lower pitch angles to higher pitch angles. Another important feature is that the SWR distribution shows a plateau region (lack of distinctly sharp peaks in the pitch angle distributions) for both maxima and minima for higher pitch angles in SC23. In contrast, conspicuous peaks are noticed in the case of SWR distribution during both maxima and minima in SC24. Despite all the above features, the green line is near zero which means there is little difference between the alpha and proton pitch angle distributions. Therefore, there is no significant difference between the pitch angle distributions of alphas

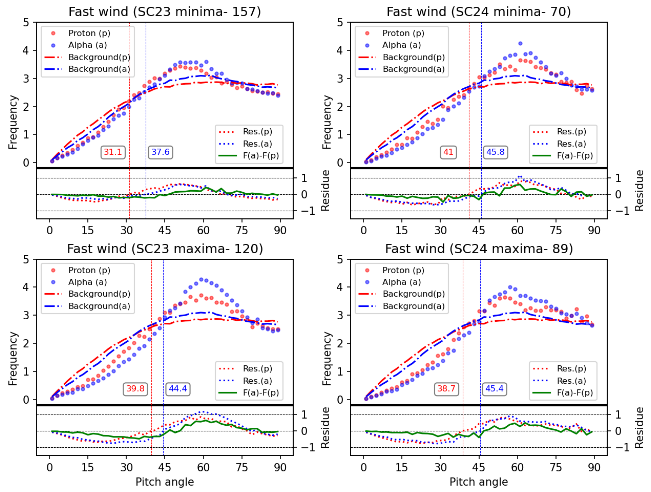

Figure 4. The pitch angle distributions for minima and maxima for SC23 and 24 are shown only for the fast wind region (FWR). The red and blue colors are used for protons and alphas, respectively. The upper part of each panel shows the pitch angle distribution for FWR of SIR and background fast wind. The lower part of each panel shows the difference between SIR pitch angle distribution and background fast wind. The green color indicates the difference between alpha and proton pitch angle distribution for FWR.

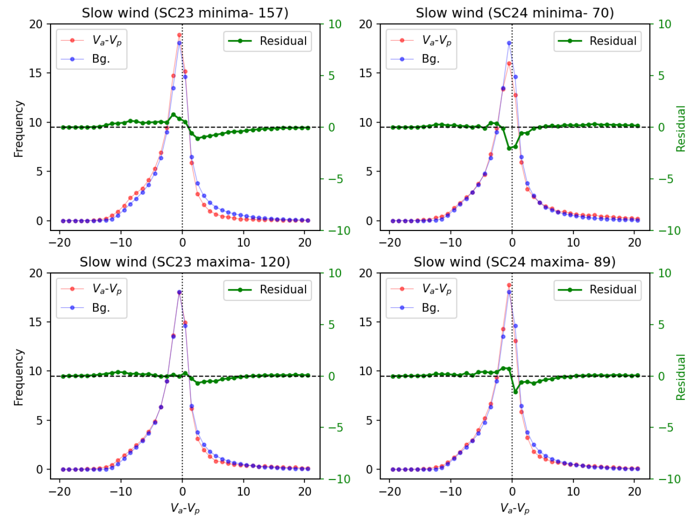

Figure 5. The distribution of differential velocity (alpha velocity – proton velocity) for minima and maxima for SC23 and 24 are shown only for the slow wind region (SWR). The red and blue colors are used for differential velocity distribution for the SWR in SIR and background (Bg.) slow wind respectively. The green color shows the difference between the slow wind region in SIR and the background slow wind distribution..

and protons in the SWR of SIR although there are higher number of protons or alpha particles for higher pitch angles than the background slow solar wind.

3.3.2 Fast Wind Region (FWR)

A similar analysis is also performed for FWR in SIR. Figure 4 is analogous to figure 3 but with the properties of FWR and background fast wind. It can be observed from figure 4 that a part of particle distribution having lower pitch angles than the background solar wind seems to have shifted towards higher values similar to SWR. However, one difference is noticed. The pitch angle distributions for FWR and background fast wind have at least two distinct crossover points unlike the slow solar wind when only one crossover point is seen. The first crossover point is at the lower pitch angle, whereas the second is at a very high value. The crossover pitch angles are nearly 40^o and 45^o for protons except for SC23 minima (31.1^o (proton) and 37.6^o (alpha)). The proton and alpha pitch angle crossover points have a difference of approximately 5^o. The alphas have higher crossover angles, suggesting that more alpha particles are shifted towards higher pitch angles. Unlike SC23, the variation in the green line (in the lower panels) in this case suggests that alphas are more at higher pitch angles than protons. This alpha and proton distribution difference is the least in the SC23 minima. Note, SC23 is characterized by a deep minimum period. Based on these results, it can be stated that the alphas behave differently than protons in the case of the FWR. In addition, the pitch angle crossovers are different from those for SWR.

3.4 Distribution of differential velocity between alphas and protons in SC23 and 24

The variation in the difference between the alpha and proton velocities (Differential velocity) are shown in Figures 5 and 6 for SWR and FWR in SC23 and 24 similar to Figures 3 and 4. Figures 5 and

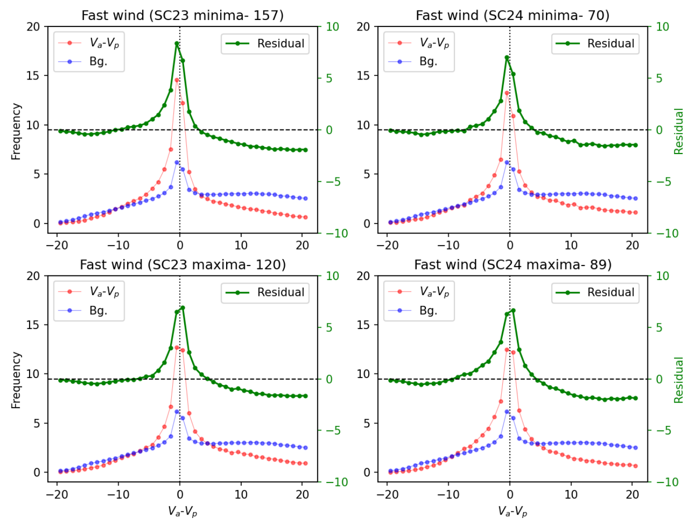

Figure 6. The distribution of differential velocity (alpha velocity – proton velocity) for minima and maxima for SC23 and 24 are shown only for the fast wind region (FWR). The red and blue colors are used for differential velocity distribution for the FWR of SIR and background (Bg.) fast wind respectively. The green color shows the difference between the fast wind region of SIR and background fast wind distribution.

6 show the distribution of velocity difference for SWR and FWR respectively. The red color in both the figures shows the differential velocity distribution for SWR and FWR for SIRs. The blue color indicates the distribution for the background differential velocity. The green color is the difference between the two distributions, i.e., differential velocity distribution for SIR and background velocity. It can be observed from figure 5 that there is hardly any difference in the distribution for SWR in SIR and in the background solar wind barring slight differences at the distribution center (V_a - V_p = 0).

The FWR distribution for differential velocity shows significant changes than the SWR distribution. The background distribution shows relatively enhanced tails towards the positive side because of the fact that alphas have higher velocity than protons in the background fast wind. Or in other words, velocities of alpha particles get reduced in the case of the FWR of SIRs. Therefore, the faster alpha particles are slowed down in the interaction region and accumulate near the center (Va=Vp) of the distribution. This is captured by the substantial enhancement of the residual curve in green near the center, suggesting the accumulation of alpha particles in the proton frame. This is the primary cause of the enhanced helium towards the FWR of SIRs.

We also note that there is little difference in the behaviours of velocity differences in the maxima and minima of SC23 and SC24. This suggests that unlike N_{He} and pitch angle, the change in the differential velocities between alphas and protons in SIRs with respect to the background solar wind is due to primarily interplanetary processes. This aspect will be discussed further in the next section.

4 DISCUSSION AND CONCLUSION

In this letter, we show that alphas and protons show different behavior in the SIRs and enhancement in A_{He} occurs across the stream interface in the fast wind region. Gosling et al. (1978) suggested that the enhancement in A_{He} at the stream interface is caused by the difference in the type (fast or slow wind having high and low A_{He} respectively) of solar wind. The SIRs can be considered as magnetic bottles or mirror assemblies (Ďurovcová et al. 2019). It is well known that the magnetic field and the velocity of the ions play important roles in controlling the bounce motion of particles. The magnetic mirror force depends on the ions' magnetic moment, m = m$V_{\perp}{}^2$/2B. This force slows down the ions or the ions having a pitch angle higher than the loss cone angle tend to have bounce-back motions. Our results suggest that alphas and protons have similar pitch angles in SWR, but in the case of FWR, more alpha particles are distributed towards higher pitch angles as compared to protons. Also, the pitch angle crossover between SIR distribution and background distribution is similar for alpha and protons for SWR. This crossover differs by approximately 5^o in the case of FWR of SIRs. This change in distribution may play an important role in causing the enhancement of alpha particles in the FWR of SIR.

In addition to pitch angle, solar wind velocity also plays a vital role in deciding the number density. In general, protons and alphas have similar speeds in the slow wind, whereas alphas are faster than protons in the fast wind. The alphas have a higher magnetic moment because of the higher velocity and mass. So, alpha particles experience more magnetic curvature or mirror force than protons. The implication of this higher force can be seen in figure 6 as the frequencies of alpha particles faster than protons are reduced in the case of FWR of SIRs. So, this difference in curvature force for alphas and proton causes a generation of the second peak of alpha particles towards FWR.

The additional important point that emerges from this work is that the SWR pitch angle distribution in SC24 shows similarities with the overall FWR pitch angle distribution as these show peaks at higher pitch angles. On the contrary, the SWR distribution in SC23 shows a plateau region at higher pitch angles. This probably indicates additional influence of the changes in the sources of slow solar wind in SC24 compared to SC23.

The above results reveal that the variations in helium abundance near the stream interface (SI) are not primarily determined by the level of solar activity. Instead, it appears that the primary factors affecting helium abundance in this region are pitch angle and differential velocity. The solar activity can determine the level of enhancement towards SWR because it changes the background value of helium abundance in the slow solar wind. This can be observed in figure 2 that the level of enhancement in helium differs in SWR whereas these levels are approximately the same in the FWR region.

In a nutshell, the SWR of SIRs does not show significant changes in pitch angle and differential velocity. This may be the primary cause behind the similar enhancement in the alphas and protons in the case of SWR. In the case of FWR, the pitch angle and differential velocity distribution show significant differences between alphas and protons. The crossover between background distribution and the FWR distribution for alphas is at a higher angle than protons. It means that more alphas are shifted towards higher pitch angles than protons, causing a significant enhancement in the alpha number density. This probably causes the second peak of alphas in the FWR. The differences in the pitch angle distribution for SC23 (plateau) and SC24 (peak) possibly indicate additional changes in the source of slow wind during SC23 and SC24. On the contrary, the differential velocities of alphas and protons do not show any significant change in SC23 and SC24. This suggest primary role of SIR in determining the differential velocities.

ACKNOWLEDGEMENTS

We thank the PIs of SWE (WIND). We acknowledge Coordinated Data Analysis Web for its open data policy. This work is supported by the Department of Space, Government of India.

DATA AVAILABILITY

The data can be obtained from `https://cdaweb.gsfc.nasa.gov/index.html/`.

REFERENCES

Alterman B. L., Kasper J. C., 2019, ApJ, 879, L6
Belcher J. W., Davis Leverett J., 1971, J. Geophys. Res., 76, 3534
Borrini G., Gosling J. T., Bame S. J., Feldman W. C., 1982, Journal of Geophysical Research: Space Physics, 87, 7370
Burlaga L. F., 1974, Journal of Geophysical Research (1896-1977), 79, 3717
Chi Y., Shen C., Luo B., Wang Y., Xu M., 2018, Space Weather, 16, 1960
Fu H., Harrison R. A., Davies J. A., Xia L., Zhu X., Li B., Huang Z., Barnes D., 2020, ApJ, 900, L18
Gosling J. T., Asbridge J. R., Bame S. J., Feldman W. C., 1978, J. Geophys. Res., 83, 1401
Hathaway D. H., 2015, Living Reviews in Solar Physics, 12, 4
Kasper J. C., Stevens M. L., Lazarus A. J., Steinberg J. T., Ogilvie K. W., 2007, ApJ, 660, 901
Laming J. M., 2004, ApJ, 614, 1063
Lepping R. P., et al., 1995, Space Sci. Rev., 71, 207
Mayank P., Vaidya B., Chakrabarty D., 2022, ApJS, 262, 23
Ogilvie K. W., et al., 1995, Space Sci. Rev., 71, 55
Richardson I. G., 2018, Living Reviews in Solar Physics, 15, 1
Richardson I. G., Cane H. V., 2010, Sol. Phys., 264, 189
Rout D., Chakrabarty D., Janardhan P., Sekar R., Maniya V., Pandey K., 2017, Geophys. Res. Lett., 44, 4532
Wimmer-Schweingruber R. F., von Steiger R., Paerli R., 1997, J. Geophys. Res., 102, 17407
Yogesh Chakrabarty D., Srivastava N., 2021, MNRAS, 503, L17
Yogesh Chakrabarty D., Srivastava N., 2022, MNRAS, 513, L106
Ďurovcová T., Němeček Z., Šafránková J., 2019, ApJ, 873, 24